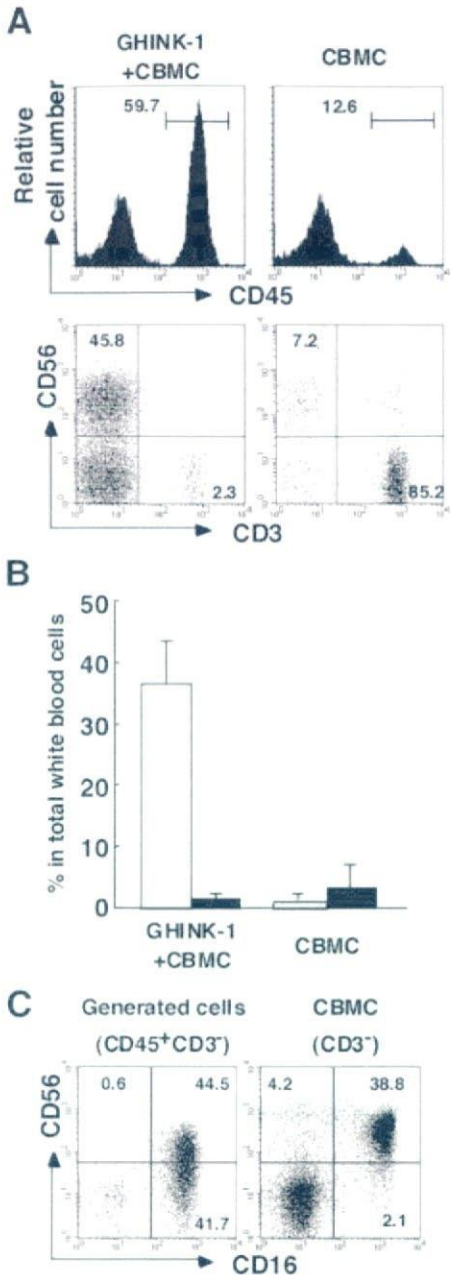

Figure 1. GHINK-1 supports the generation of human NK cells in NOD/SCID mice. CBMC with or without irradiated GHINK-1 cells were injected intraperitoneally into NOD/SCID mice. After 12 days, PB was drawn from the mice, and leukocytes were stained with anti-human CD3- or CD16-FITC, CD56-PE and CD45-PC5 mAb, and analyzed. (A) Flow cytometry of CD3 and CD56 expression on $CD45^+$ cells generated in PB of NOD/SCID mice. Numbers indicate percentage of positive cells. (B) Percentages of typical mature $CD3^-CD56^+$ NK cells (blank bar) and $CD3^+CD56^-$ T cells (solid bar) in PB were compared among mice injected with CBMC plus GHINK-1 (n=8), and CBMC alone (n=6). Bars show standard deviation. (C) Flow cytometry of CD16 and CD56 expression in PB of the transplanted NOD/SCID mice (within $CD45^+CD3^-$ cells, left) and primary human CBMC (except $CD3^+$ cells, right). One set of representative results from three independent experiments is shown.

fluorescent vital dye CFSE. CBMC were labeled with CFSE to assess NK cell development and proliferation *in vivo* by a standard flow cytometry-based assay [35], and transplanted with GHINK-1 cells into NOD/SCID mice. At day 7 post transplantation, cells were harvested from PB and analyzed. A reduction in CFSE was observed in $CD3^-CD56^+$ NK cells (Fig. 3A, upper left). In contrast, the division numbers of $CD3^+CD56^-$ T cells were far smaller than that of $CD3^-CD56^+$ NK cells, and its rate was the same as those in CBMC-transplanted mice (data not shown). Next, the proliferation of NK cells was investigated *in vitro*. CFSE-labeled CBMC was co-cultured with GHINK-1 cells in the absence of IL-2. At day 7 of culture, cells were harvested and analyzed for CFSE intensity. $CD3^-CD56^+$ NK cells proliferated in the co-culture of CBMC and GHINK-1 cells, but not in the culture of CBMC (Fig. 3A, upper middle). No evidence of cell division, *i.e.*, dilution of CFSE was observed in $CD3^+CD56^-$ T cells in either culture (Fig. 3A, lower middle and right). These results together with those of the *in vivo* experiments (Fig. 3A, lower left) indicate that GHINK-1 could support the proliferation of $CD3^-CD56^+$ NK cells but not $CD3^+CD56^-$ T cells.

To further characterize the function of GHINK-1 cells for the NK cell proliferation, we cultured CFSE-labeled CBMC with GHINK-1 in the presence or absence of IL-2. IL-2 induced the proliferation of $CD3^-CD56^+$ NK cells with a significant up-regulation of activation markers, NKp44 and CD69 (Fig. 3B). On the other hand, GHINK-1 alone induced the proliferation of $CD3^-CD56^+$ NK cells without the up-regulation of NKp44 and CD69. Interestingly, GHINK-1 partially suppressed the up-regulation of NKp44 and CD69 by IL-2 stimulation. Thus, GHINK-1 supports the proliferation of NK cells without activation *in vitro*.

NK cells generated in NOD/SCID mice exhibit a resting phenotype

Further phenotyping was performed for the expression of NK cell-specific cell surface markers on $CD16^+$ NK cells. PB leukocytes were harvested from the mice at day 14 after the co-transplantation, and the expression pattern was compared with that of NK cells freshly isolated from human CB (resting NK cells) and IL-2-activated NK cells. The NK cells generated in NOD/SCID mice expressed CD56, CD94, CD161, NKG2D, NKp30 and NKp46 (NKRs) (Fig. 4A). CD2 (co-stimulatory molecule) showed a heterogenous expression pattern in the NK cells generated in the mice as well as resting and activating NK cells. In addition, other NK cell-related markers such as CD7 (co-stimulatory molecule), CD11a (adhesion molecule), DNAM-1 (activating receptor) and NKB1 (inhibitory receptor) were also detected (data not shown). By contrast, activation markers, CD25, CD69

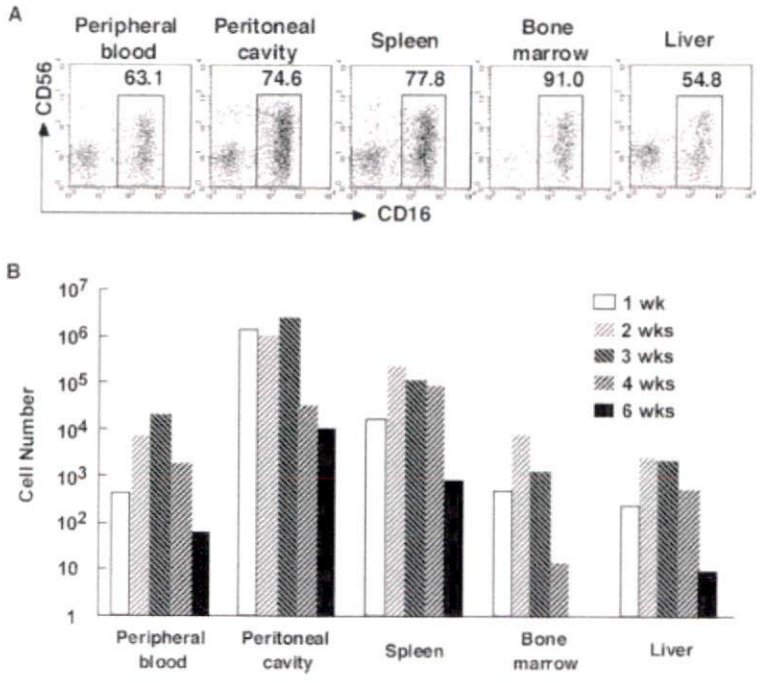

Figure 2. Engraftment of human NK cells in the hematopoietic organs of NOD/SCID mice. Cells were harvested from PB, peritoneal cavity, spleen, bone marrow, and liver of NOD/SCID mice at the indicated time after co-transplantation of GHINK-1 cells and CBMC. Human $CD45^+$ cells were further analyzed for the expression of CD16 and CD56 by flow cytometry. (A) The expression of CD16 and CD56 was analyzed on $CD45^+$ cells by flow cytometry at 1 week after the transplantation. Numbers indicate percentage of NK cells in human leukocytes. (B) Time course of total NK cell number in various sites of the transplanted mice. Absolute NK cell numbers were calculated by multiplication of absolute white blood cell number and percentage of NK cell at the indicated time. The values of PB mean cells per 1 mL of PB. The values of peritoneal cavity and bone marrow are from total peritoneal fluid and two femurs, respectively. The values of spleen and liver are for whole organs. One set of representative results from three independent experiments is shown.

and NKp44 were only slightly expressed on the vast majority of NK cells generated in the mice, likely as freshly isolated resting NK cells (Fig. 4B). Cell size and granularity were analyzed in $CD16^+$ cells using FSC/SSC dot blots, and were also similar to those in resting NK cells (Fig. 4C). These results indicated that the NK cells generated in the mice were not activated, but resting NK cells, which exist in the PB and CB.

Human NK cells generated in NOD/SCID mice can be activated by stimulation with IL-2

Human resting NK cells are known to activate and augment the expression of adhesion molecules, activation markers and cytotoxicity by IL-2 [26, 27, 36, 37]. We examined whether the NK cells from NOD/SCID mice also augment the expression of CD56 and activation markers induced by IL-2. The NK cells were harvested from the peritoneal cavity of the co-transplanted mice, and the expression of CD56, the early activation marker CD69, and the activated NK cell receptor, NKp44 [38], were analyzed 14 days after culture with IL-2. Expression of CD56, CD69 and NKp44 were weak or absent in the pre-culture (Fig. 5A, left panels). After the culture with IL-2, the expression of CD56, CD69 and NKp44 was clearly augmented (Fig. 5A, right panels), indicating that the generated NK cells were activated by stimulation with IL-2. Next, $CD56^-CD16^+$ and $CD56^+CD16^+$ fractions were sorted using flow cytometry and cultured with IL-2 as above. Expression of CD56 was also augmented in both populations (Fig. 5B), indicating that $CD56^-CD16^+$ cells are possible precursors of mature $CD56^+CD16^+$ NK cells as described [32–34], but $CD56^{bright}CD16^-$ cells were not generated from $CD56^-CD16^+$ cells in this culture. Thus, the newly generated NK cells had the ability to express CD56, activation markers and cytotoxicity after activation by IL-2, which is identical to the resting NK cells in human PB.

Cytotoxic activity and antitumor effects of the NK cells generated in NOD/SCID mice

The most important characteristic of NK cells is the capacity to kill target cells without prior sensitization. To evaluate the cytotoxic activity of NOD/SCID mice derived human NK cells, we used an HLA class I-deficient human erythroleukemia cell line, K562, which is commonly used as a sensitive NK cell target *in vitro* and on subcutaneous inoculation *in vivo* [20, 39]. For the analysis of K562 cell lysis *in vitro*, freshly isolated and IL-2-stimulated NK cells were co-cultured with EGFP-K562, and their cytotoxicity was measured by flow cytometry [40]. Both the freshly isolated and IL-2-stimulated NK cells showed cytotoxicity, but the activity of activated NK cells was approximately tenfold that of freshly isolated *in vivo*-generated NK cells as expected (Fig. 6).

Finally, we evaluated the antitumor activity of the *in vivo*-generated NK cells. CBMC plus GHINK-1, CBMC or GHINK-1 cells were transplanted into NOD/SCID mice. After 8 days, the mice were inoculated subcutaneously with K562 cells. After 2 wks, tumor size was significantly suppressed in the mice co-transplanted with CBMC and GHINK-1 cells than in the mice transplanted with GHINK-1 cells or CBMC ($p=0.018$ and $p=0.009$,

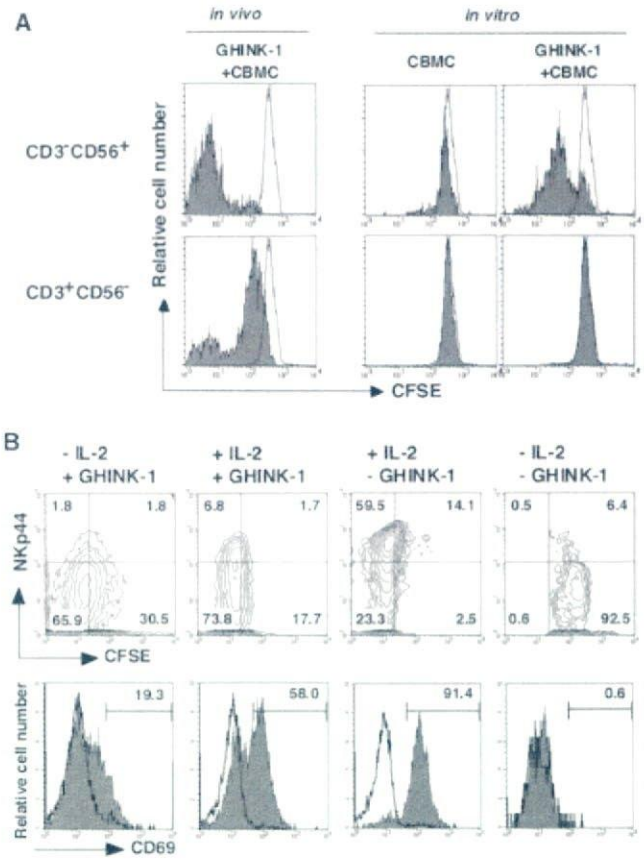

Figure 3. GHINK-1 cells induce selective proliferation of human NK cells *in vitro* and *in vivo* without exogenous IL-2. (A) CFSE-labeled CBMC were intraperitoneally injected with GHINK-1 cells into NOD/SCID mice, or cultured with or without GHINK-1 cells *in vitro*. After 7 days, the cells were harvested and stained with anti-CD56-PE and CD3-PC5 mAb, and fluorescence intensity of CFSE was analyzed on $CD3^-CD56^+$ and $CD3^+CD56^-$ cells. Open profiles indicate non-divided cells. (B) CFSE-labeled or unlabeled CBMC was co-cultured under indicated conditions. Cells were stained with anti-CD3-PE/Cy7, CD56-PC5 and NKp44-PE, or anti-CD69-FITC, CD3-APC and CD56-PE8. CFSE reduction and expression of NKp44 and CD69 on $CD3^-CD56^+$ NK cells were analyzed by flow cytometry at day 5. Numbers indicated percentage of the cells in each fraction. One set of representative results from three independent experiments is shown.

respectively), while there was no significant difference between GHINK-1 -transplanted and CBMC-transplanted mice ($p=0.5$) (Fig. 7A). Subsequently, we performed immunohistochemistry to detect $CD16^+$ cells in the tumor tissues of the co-transplanted mice. $CD16^+$ cells were observed in the tumor tissues, particularly, around necrotic tumor cells (Fig. 7B). These results suggested that the human NK cells migrated to tumor cells and killed them *in vivo*.

Discussion

In this study, we established a mouse model that engrafted human NK cells. Human NK cells were selectively generated in NOD/SCID mice with intraperitoneal co-transplantation of CBMC and GHINK-1, a cell line that selectively stimulates human NK cell proliferation. Two human NK cell populations, cytotoxic $CD56^{dim}CD16^+$ and immature $CD56^-CD16^+$ cells, appeared in PB and other hematopoietic organs of the mice. Most of the NK cells generated did not express activation markers (CD25 and CD69) or the activated NK cell marker (NKp44), indicating that they are resting NK cells resembling human PB and CB NK cells. These NK cells were activated by stimulation with IL-2, and showed antitumor effects both *in vivo* and *in vitro*. Thus, the NK cells generated in this system are functionally and phenotypically identical to those in human PB. The mouse model provides information about the dynamics of physiological NK cells *in vivo* and an important preclinical evaluation system for immunotherapeutic strategies.

Our understanding of the development and function of human NK cells is largely based on *in vitro* analysis, and appropriate models to study human NK cells *in vivo* have been lacking. The NOD/SCID mouse was found to be an efficient recipient for the reconstitution of human hematopoietic cells. However, the lymphoid differentiation is restricted to the B cell lineage [13], and T and NK cells are produced at a minimum level even in modified strains like NOD/SCID β2-microglobulin-deficient [14] or NOD/SCID common γc-deficient mice [18]. Recently, Kalberer *et al.* [20] reported engraftment of human NK cells on administration of IL-15 and Flt-3 ligand into $CD34^+$ cell-transplanted NOD/SCID mice. In their model, the administration of these growth factors specifically generated mature $CD56^+$ NK cells and $CD34^-CD7^+$ NK precursor cells in bone marrow and spleen over a long period (more than 5 months). A number of studies have now demonstrated that human NK cells can be generated *in vitro* from $CD34^+$ hematopoietic stem cells in cultures that contain key cytokines (IL-2, IL-12, IL-15 etc.) and multi-lineage hematopoietic growth factors (SCF and Flt-3 ligand) [21–24]. On the other hand, stroma cells are said to play an important role in NK cell development [41]. Although some stroma cell molecules can be replaced by cytokines such as SCF, Flt3-ligand and IL-15 [21–24], we have recently demonstrated that a Wilms' tumor cell line, HFWT (original strain of GHINK-1 cells), can stimulate the differentiation of mature NK cells from Lin^-CD122^+ NK precursors, but not from $CD34^+$ hematopoietic stem cells [34]. Thus, cell-to-cell interaction is essential for the generation of NK cells and soluble factors such as IL-15 are not involved in this process [29]. This represents

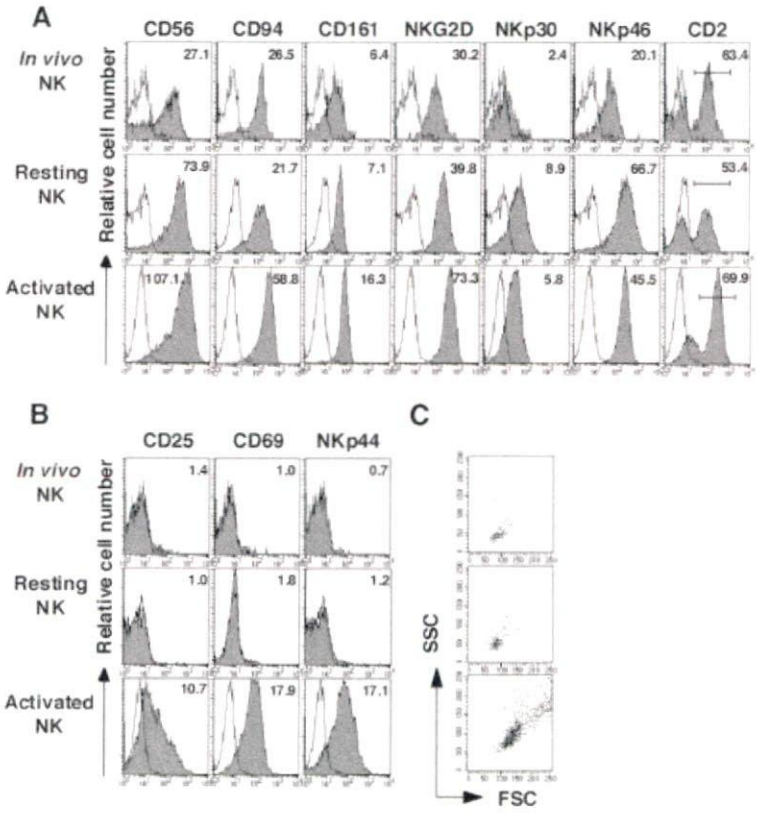

Figure 4. Surface antigen expression on the NK cells generated in NOD/SCID mice. NK cells generated in NOD/SCID mice (day 12 after the co-transplantation) (*In vivo* NK), freshly isolated CBMC (Resting NK), and CBMC cultured *in vitro* with GHINK-1 cells and IL-2 for 10–14 days (Activated NK) were stained with the indicated mAb and analyzed on $CD16^+$ cells by flow cytometry. (A) CD94, CD161, NKG2D, NKp30, NKp46 and CD2 are the NK cell receptors and costimulatory molecule, respectively. Numbers in CD2 show percentages of positive cells, and others show relative mean fluorescence intensity (monoclonal antibody/negative control). (B) CD25, CD69 and NKp44 are activation markers. Open profiles indicate negative control. (C) FSC/SSC dot plot indicates cell size and granularity. One set of representative results from three independent experiments is shown.

the phenotypic differences of the mice. In the study of Kalberer *et al.*, cytokine-induced NK cells mainly consist of $CD56^+CD16^+$ cells that express the activation marker CD69. In contrast, our GHINK-1-generated NK cells are $CD56^{dim}CD16^+$ and $CD56^-CD16^+$ NK cells with the resting phenotype. This discrepancy can be explained by the notion that IL-15 works as a potent activator of NK cells as well as NK cell development, whereas cell-to-cell contact may provide both proliferative signals and inhibitory signals for activation. This is in agreement with the fact that hematopoietic stem cells proliferate but differentiate in the presence of soluble cytokines, while they proliferate and self renew in the presence of stroma cells. Thus, stroma cells or the microenvironment appropriately regulate the development and function of hematopoietic cells through a balance of positive and negative signals. One important molecule that interacts between hematopoietic stem cells and stroma cells is CXCR4 and its ligand SDF-1 [42]. NK cells also express CXCR4 [43], and Beider *et al.* [19] showed that CXCR4 is heavily involved in the homing and retention of human NK and NKT cells at the bone marrow and spleen of NOD/SCID mice. Following activation with IL-2, the levels of CXCR4 on NK and NKT cells decreased significantly, and inhibited the homing and retention in the bone marrow and spleen of NOD/SCID mice [19]. Thus, stroma cells regulate the development and function of NK cells. In this study, we revealed that GHINK-1 cells stimulate proliferation of resting NK cells without activation both *in vivo* and *in vitro* (Fig. 3, 4). Ferlazzo *et al.* [44] reported that human DC also stimulates proliferation of resting NK cells with slight increases of activating markers expression. It is possible that a putative ligand for resting NK cell stimulation expressed on DC is also expressed on GHINK-1 cells, and that the ligand on GHINK-1 cells reacts with unknown receptors selectively expressed on NK cells. In this context, the identification of responsible molecules on GHINK-1 feeder cells will enable us to clarify the regulatory mechanisms of NK cell development and function.

Human PBMC contain approximately 10% NK cells [1]. Subsets of NK cells in adult PBMC can be distinguished by the surface density of CD56 antigen as well as by the presence or absence of CD16 antigen. The majority are $CD56^{dim}CD16^+$, the most cytotoxic subset. A minor NK subset in PB is formed by $CD56^{bright}CD16^-$ cells, which produce a series of cytokines including IFN-γ, TNF-α, GM-CSF, and IL-10 upon activation, while $CD56^{dim}CD16^+$ NK cells produce few of these cytokines [5]. There are few $CD56^-CD16^+$ NK cells in adults, but they have been identified in CB as possible precursors of mature $CD56^+$ NK cells, which, when cultured in the presence of IL-2, IL-12, or IL-15, acquire adult-like cytotoxic activity and cytokine production [33, 34]. The NK cells generated *in vivo*

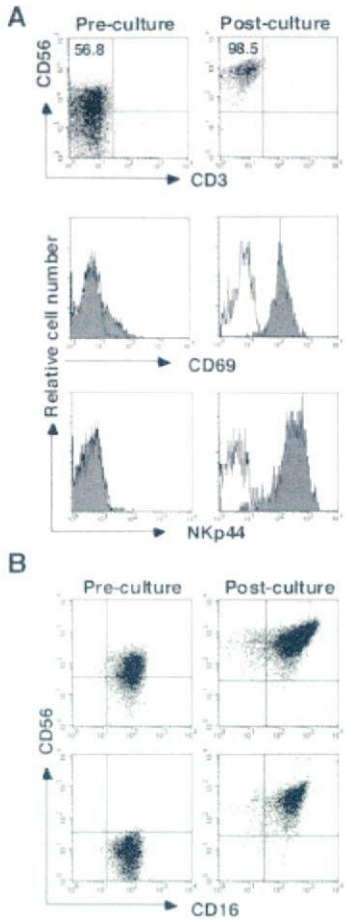

Figure 5. *In vitro* activation of human $CD56^{dim}CD16^{+}$ and $CD56^{-}CD16^{+}$ NK cells derived from NOD/SCID. Cells were harvested from the peritoneal cavity of NOD/SCID mice at day 12 after the co-transplantation, and investigated for the expression of cell surface markers. (A) Expression of CD3 and CD56 on $CD45^{+}$ cells, and CD69 or NKp44 on $CD16^{+}$ cells. Open profiles indicate the negative control. (B) Expression of CD56 on purified $CD56^{dim}CD16^{+}$ and $CD56^{-}CD16^{+}$ cells. Freshly isolated cells (Pre-culture, left panels) were cultured with IL-2 for 14 days (Post-culture, right panels). One set of representative results from three independent experiments is shown.

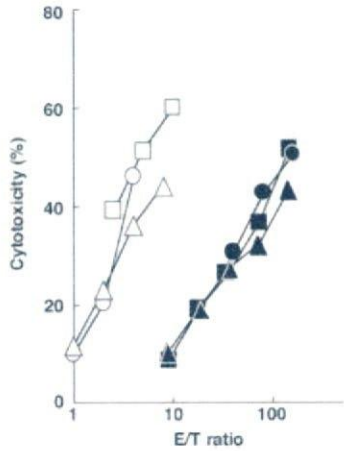

Figure 6. Cytotoxicity of human NK cells from NOD/SCID mice is augmented by IL-2. Cells were harvested from the peritoneal cavity of NOD/SCID mice at day 12 after the co-transplantation. They were assayed for cytotoxicity immediately (closed symbols), or after cultivation with IL-2 for 10–14 days (open symbols). The effector cells were co-cultured with EGFP-K562 target cells at the indicated E/T ratios. After 6-h incubation, PI was added to the cell mixture, and cytotoxicity was measured by flow cytometry. Cytotoxicity was calculated from percentages of PI^{+} and $EGFP^{+}$ cells as described in Materials and Methods. Three different symbols represent three independent experiments from three donors.

consisted of $CD56^{dim}CD16^{+}$ and $CD56^{-}CD16^{+}$ cells but not $CD56^{bright}CD16^{-}$ NK cells in our model. In contrast, in the study of Kalberer *et al.*, the growth factor-treated mice predominantly generated $CD56^{bright}CD16^{-}$ cells [20]. These results suggest that the development of $CD56^{dim}CD16^{+}$ and $CD56^{bright}CD16^{-}$ cells requires different molecules. It has previously been suggested that $CD56^{bright}CD16^{-}$ cells are precursors of $CD56^{dim}CD16^{+}$ cells [45], but the finding that our GHINK-1-treated mice had no $CD56^{bright}CD16^{-}$ cells and that $CD56^{-}CD16^{+}$ immature NK cells could differentiate into the $CD56^{dim}CD16^{+}$ NK cells [34] (Fig. 5B) support that $CD56^{bright}CD16^{-}$ cells are not the direct precursors of $CD56^{dim}CD16^{+}$ NK cells. Thus, our model mice provide information about NK cell development as well as the function of the main NK population in human PB ($CD56^{dim}CD16^{+}$).

NK cells are innate immune lymphocytes, which showed early clinical promise because of their ability to lyse tumor cells without specific antigen recognition. Clinical trials attempting to harness the antitumor effect of NK cells, either through *in vivo* or *in vitro* activation [46–48], however, have met with only modest success to date. These trials were based on *in vitro* cytotoxicity or activated NK cell-mediated antitumor activity in the mouse model, and their experimental results did not directly link to clinical stages. The next immunotherapeutic strategies will be to modify resting NK cell functions. For example, chemokine gene transduction into tumor cells to enhance recruitment of NK cells or tumor-specific mAb treatment to induce antibody-dependent cellular cytotoxicity (ADCC), which is mediated through CD16 on cytotoxic $CD56^{dim}$ NK cells may be a good candidate for immunotherapy using NK cells. However, such pre-clinical examinations could not be performed, because no suitable animal model is available that has steady-state "resting" human NK cells. In the present study, the human NK cells of NOD/SCID origin showed an identical phenotype to resting (blood circulating) $CD56^{dim}CD16^{+}$ NK cell (Fig. 4) and cytotoxic activity *in vitro* (Fig. 6), and are capable of reducing K562 erythroleukemia tumor formation *in vivo* (Fig. 7). Therefore, our present model mouse has functional and physiologically resting NK cells. This

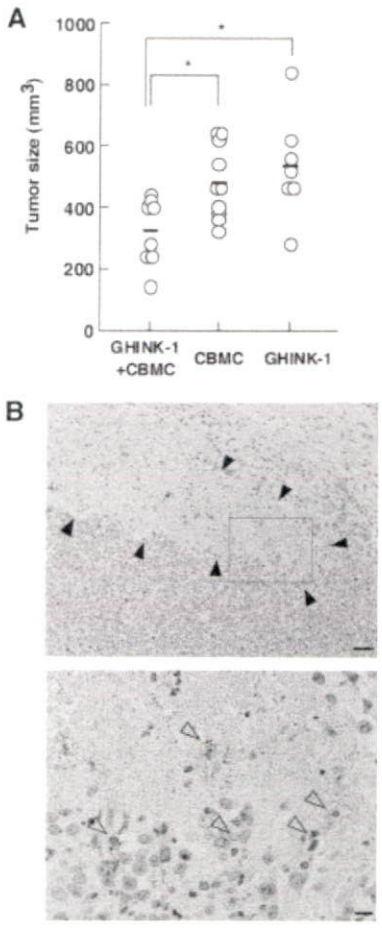

Figure 7. The NK cells generated in mice exhibit antitumor activity and infiltrate into the tumor tissues. (A) K562 cells were injected subcutaneously into the right flank of NOD/SCID mice. Eight days later, CBMC and GHINK-1, CBMC or GHINK-1 cells were injected into peritoneal cavity of the mice. Tumor size (mm^3) was measured at day 14 after the injection of K562 cells. Data for each group were obtained from seven to ten mice. (B) Human NK cells infiltrated K562 tumor tissue. CBMC and GHINK-1 cells were co-transplanted into NOD/SCID mice, and K562 cells were injected subcutaneously into the mice as described in Materials and Methods. After 14 days, the tumor tissues were subjected to immunohistochemistry with anti-CD16 mAb and visualized with 3,3′-diaminobenzidine. Regions within closed triangles are necrotic tumor tissue (upper panel). The lower panel shows a close-up of part of the upper panel. Open triangles show $CD16^+$ cells. Scales in upper and lower panels represent 40 and 10 μm, respectively.

model mouse will be useful for pre-clinical study of NK cell-based immunotherapies.

The translation of NK cell biology to the clinic should result in a significant improvement of NK-cell based therapies for cancer. Our mice represent an important model for evaluation of the immunotherapeutic efficacy of human NK cells and for investigations of the factors and signals orchestrating (coordinating) the formation of the NK cell compartment in humans.

Materials and methods

CB, cell lines and culture

CB was kindly provided by Fukuda Hospital (Kumamoto, Japan) with the informed consent of the mothers. Investigations were approved by the Ethical Committee of the Kumamoto University Graduate School of Medical Science. CBMC were separated by LSM lymphocyte separation medium (Cappel, Aurora, OH) density-gradient centrifugation for use in the *in vitro* and *in vivo* experiments.

A subline of the Wilms' tumor cell line HFWT, GHINK-1, was established and maintained in DMEM (Sigma, St. Louis, MO) supplemented with 10% heat-inactivated FBS [30]. The K562 cell line was obtained from RIKEN Cell Bank (Tsukuba, Japan). EGFP-transfected K562 (EGFP-K562) cells were established with pEGFP-N1 (BD Biosciences, San Diego, CA) and the transfection reagent Fugene 6 (Roche, Indianapolis, IN) according to the manufacturer's instruction manual. Original and EGFP-K562 cell lines were cultured in RPMI 1640 medium (Sigma) supplemented with 10% FBS.

CBMC were cultured with or without irradiated GHINK-1 cells in RPMI 1640 medium (Sigma) supplemented with 10% autologous plasma without IL-2 (Shionogi Chemical Institute, Osaka, Japan) for 7 days. Engrafted human cells in the peritoneal cavity of NOD/SCID mice were cultured in the above medium with 200 U/mL IL-2 for 10–14 days. Activated NK cells were obtained by culturing CBMC and irradiated (50 Gy) GHINK-1 cells with 200 U/mL of IL-2 for 10–14 days as previously described [27].

Mice and transplantation

NOD/SCID mice purchased from Clea Japan (Tokyo, Japan) were bred and maintained in laminar flow housing at the Center for Animal Resources and Development (CARD), Kumamoto University. NOD/SCID mice, 8–12 weeks old, were irradiated (2.5 Gy) and 3×10^7 CBMC with or without 3×10^6 irradiated (50 Gy) GHINK-1 cells were injected intraperitoneally. After transplantation, leukocytes were harvested from PB, peritoneal cavity, spleen, bone marrow and liver for further analysis. Red blood cells were lysed with red cell lysing buffer (155 mM NH_4Cl, 10 mM $KHCO_3$, and 0.1 mM EDTA). In the case of liver, homogenized specimens were passed through a cell strainer (70 μm) and mononuclear cells were obtained by density-gradient centrifugation as described above. All of the animal experiments were performed according to the guidelines of Kumamoto University, Graduate School of Medical Science.

Flow cytometry and cell sorting

FITC-labeled anti-CD16 (3G8), -CD69 (FN50), -CD94 (HP-3D9), -CD161 (VI NK12), -DNAM-1 (DX11), -NKB1 (DX9), PE-labeled anti-CD7 (M-T701), -CD56 (B159) and -CD25 (M-A251) were purchased from BD PharMingen (San Diego, CA). FITC-labeled anti-CD2 (G11), -CD3 (S4.1) and PE-Cy5 (PC5)-labeled anti-CD45 (HI30) were provided by Caltag (Burlingame, CA). PE-labeled anti-CD11a (25.3), -NKG2D (ON72), -NKp30 (Z25), -NKp44 (Z231), -NKp46 (BAB281) and PC5-

labeled anti-CD3 were obtained from Beckman Coulter (Fullerton, CA). Isotype-matched control mAb were used as negative controls. Cells were treated with red cell lysing buffer to lyse erythrocytes before staining. Single-cell suspensions were prepared in staining medium (PBS with 3% FBS and 0.05% sodium azide), and stained with the mAb described above. After a 30-min incubation on ice, cells were washed twice, resuspended in staining medium, and immediately analyzed on a FACScan flow cytometer (Becton Dickinson, San Jose, CA). Cell proliferation was observed using CFSE fluorescence labeling reagent (Molecular Probes, OR). Staining was conducted according to the manufacture's instructions. CFSE-labeled CBMC were further stained with anti-CD56-PE and anti-CD3-PC5 mAb as described above. $CD45^+CD56^{-\text{ or dim}}$ $CD16^+$ cells from the peritoneal cavity of the mice were sorted on a JSAN flow cytometer (Bay Bioscience, Japan).

Cytotoxicity assay

The cytotoxic activity of the NK cells was measured by flow cytometry with EGFP-K562 cells as described by Kantakamalakul *et al.* [40]. Briefly, 50-μL aliquots of EGFP-K562 cells (1×10^5 cell/mL) were placed in 5-mL round-bottom tubes, and 400 μL twofold serial diluted effector cells was added. Effector alone was used as a negative control. After a 6-h incubation at 37°C, 50 μL 20 μg/mL propidium iodide (PI) was added with incubation for an additional 15 min. Target cells in FSC (forward scatter) *vs.* SSC (side scatter) dot plots were gated, and GFP and PI were measured by FACScan. Cytotoxic activity was calculated as follows: $[A/(A+B) \times 100] - C$ (%), where A is the percentage of PI^+EGFP^+ cells; B is the percentage of PI^-GFP^+ cells at each E/T ratio; C is the percentage of spontaneous PI^+ cells without effector cells $[A/(A+B) \times 100$ (%) at E/T ratio $=0]$.

Antitumor activity *in vivo* (K562 tumor formation)

K562 cells (1×10^6 cells/mouse) were transplanted subcutaneously into the right flank of the NOD/SCID mice at day 8 after the intraperitoneal injection of CBMC and GHINK-1 cells, CBMC alone, or GHINK-1 cells alone. Tumor growth was monitored by measuring maximal and minimal diameters with calipers every 3–4 days, and tumor size was estimated with the formula: tumor size (mm^3) = length (mm) × $width^2$ (mm) × 0.4 as described previously [49]. The effect of NK cells on tumor growth was determined in groups of seven to ten mice. For immunohistochemistry, CBMC with or without GHINK-1 cells were injected simultaneously with the subcutaneous injection of K562 cells. After 14 days, the tumor tissues were subjected to immunohistochemistry.

Immunohistochemistry

Tumor tissues were removed from the mice and fixed with 10% formalin. The tumor specimens were embedded in paraffin. Paraffin sections, 4 μm thick, were deparaffinized through graded ethanol and rehydrated in distilled water. Endogenous peroxidase was inhibited by a 30-min incubation in methanol containing 0.3% H_2O_2. To optimize immunodetection, nonenzymatic antigen unmasking was performed by heating tissue sections for 10 min in a microwave in 5 mM citrate buffer (pH 6). After cooling, sections were incubated with normal goat serum (Nichirei, Tokyo, Japan) diluted in PBS containing 1% BSA for 30 min. Incubation with the anti-CD16 (2H7) mAb (Novocastra, Newcastle-upon-Tyne, UK) was performed overnight at 4°C. Sections were subsequently rinsed three times in PBS with Triton X-100, and treated with biotinylated goat anti-mouse immunoglobulin (Nichirei) for CD16 staining. After rinsing, the sections were incubated with streptavidin-horseradish peroxidase complex (Nichirei) for 30 min and finally visualized with the use of 3,3′-diaminobenzidine (DAKO, Glostrup, Denmark) in 0.05 M acetate buffer containing 0.015% H_2O_2. The slides were counterstained with hematoxylin. As positive control for CD16 immunostaining, paraffin sections of human tonsil were processed using the same immunostaining procedures, and as a negative control, the same staining method was carried out without the antisera.

Statistical analysis

The statistical significance of differences was determined using Student's *t*-test. *p* values less than 0.05 were defined as statistically significant.

Acknowledgements: We are grateful to Dr. Matsui and his coworkers (Fukuda Hospital, Kumamoto, Japan) for providing human umbilical cord blood, Dr. Ohno (Cell-Medicine Inc., Japan) for providing GHINK-1 cells, Ms. Y Endo for secretarial assistance, and Ms. R Shimamura for skillful technical assistance. This work was supported in part by Health and Labour Sciences Research Grants from the Ministry of Health, Labour and Welfare of Japan.

References

1 **Robertson, M. J. and Ritz, J.**, Biology and clinical relevance of human natural killer cells. *Blood* 1990. **76:** 2421–2438.

2 **Ljunggren, H. G. and Karre, K.**, In search of the 'missing self': MHC molecules and NK cell recognition. *Immunol. Today* 1990. **11:** 237–244.

3 **Moretta, L., Bottino, C., Pende, D., Mingari, M. C., Biassoni, R. and Moretta, A.**, Human natural killer cells: their origin, receptors and function. *Eur. J. Immunol.* 2002. **32:** 1205–1212.

4 **French, A. R. and Yokoyama, W. M.**, Natural killer cells and viral infections. *Curr. Opin. Immunol.* 2003. **15:** 45–51.

5 **Cooper, M. A., Fehniger, T. A. and Caligiuri, M. A.**, The biology of human natural killer-cell subsets. *Trends Immunol.* 2001. **22:** 633–640.

6 **Herberman, R. B.**, Cancer immunotherapy with natural killer cells. *Semin. Oncol.* 2002. **29:** 27–30.

7 **Wu, J. and Lanier, L. L.**, Natural killer cells and cancer. *Adv. Cancer Res.* 2003. **90:** 127–156.

8 **Ravetch, J. V. and Lanier, L. L.**, Immune Inhibitory receptors. *Science* 2000. **290:** 84–89.

9 **Moretta, A., Biassoni, R., Bottino, C., Mingari, M. C. and Moretta, L.**, Natural cytotoxicity receptors that trigger human NK-cell-mediated cytolysis. *Immunol. Today* 2000. **21:** 228.

10 **Lanier, L. L.**, On guard- activating NK cell receptors. *Nat. Immunol.* 2001. **2:** 23–27.

11 **Biassoni, R., Cantoni, C., Pende, D., Sivori, S., Parolini, S., Vitale, M., Bottino, C. and Moretta, A.,** Human natural killer cell receptors and co-receptors. *Immunol. Rev.* 2001. **181:** 203–214.

12 **Moretta, L., Bottino, C., Pende, D., Vitale, M., Mingari, M. C. and Moretta, A.,** Different checkpoints in human NK-cell activation. *Trends Immunol* 2004. **25:** 670–676.

13 **Hogan, C. J., Shpall, E. J., McNulty, O., McNiece, I., Dick, J. E., Shultz, L. D. and Keller, G.,** Engraftment and development of human $CD34^+$-enriched cells from umbilical cord blood in NOD/LtSz-*scid/scid* mice. *Blood* 1997. **90:** 85–96.

14 **Kollet, O., Peled, A., Byk, T., Ben-Hur, H., Greiner, D., Shultz, L. and Lapidot, T.,** β2microglobulin-deficient ($\beta2m^{null}$) NOD/SCID mice are excellent recipients for studying human stem cell function. *Blood* 2000. **95:** 3102–3105.

15 **Shultz, L. D., Lang, P. A., Christianson, S. W., Gott, B., Lyons, B., Umeda, S. Leiter, E.** *et al.*, NOD/LtSz-Rag1null mice: an immunodeficient and radioresistant model for engraftment of human hematolymphoid cells, HIV infection, and adoptive transfer of NOD mouse diabetogenic T cells. *J. Immunol* 2000. **164:** 2496–2507.

16 **Christianson, S. W., Greiner, D. L., Hesselton, R. A., Leif, J. H., Wagar, E. J., Schweitzer, I. B., Rajan, T. V.** *et al.*, Enhanced human $CD4^+$ T cell engraftment in beta2-microglobulin-deficient NOD-scid mice. *J. Immunol* 1997. **158:** 3578–3586.

17 **van Rijn, R. S., Simonetti, E. R., Hagenbeek, A., Hogenes, M. C., de Weger, R. A., Canninga-van Dijk, M. R., Weijer, K.** *et al.*, A new xenograft model for graft-versus-host disease by intravenous transfer of human peripheral blood mononuclear cells in $RAG2^{-/-}$ $\gamma c^{-/-}$ double-mutant mice. *Blood* 2003. **102:** 2522–2531.

18 **Hiramatsu, H., Nishikomori, R., Heike, T., Ito, M., Kobayashi, K., Katamura, K. and Nakahata, T.,** Complete reconstitution of human lymphocytes from cord blood $CD34^+$ cells using the NOD/SCID/γc^{null} mice model. *Blood* 2003. **102:** 873–880.

19 **Beider, K., Nagler, A., Wald, O., Franitza, S., Dagan-Berger, M., Wald, H., Giladi, H.** *et al.*, Involvement of CXCR4 and IL-2 in the homing and retention of human NK and NK T cells to the bone marrow and spleen of NOD/SCID mice. *Blood* 2003. **102:** 1951–1958.

20 **Kalberer, C. P., Siegler, U. and Wodnar-Filipowicz, A.,** Human NK cell development in NOD/SCID mice receiving grafts of cord blood $CD34^+$ cells. *Blood.* 2003. **102:** 127–135.

21 **Silva, M. R., Hoffman, R., Srour, E. F. and Ascensao, J. L.,** Generation of human natural killer cells from immature progenitors does not require marrow stromal cells. *Blood* 1994. **84:** 841–846.

22 **Shibuya, A., Nagayoshi, K., Nakamura, K.. and Nakauchi, H.,** Lymphokine requirement for the generation of natural killer cells from $CD34^+$ hematopoietic progenitor cells. *Blood* 1995. **85:** 3538–3546.

23 **Mrozek, E., Anderson, P. and Caligiuri, M. A.,** Role of interleukin-15 in the development of human $CD56^+$ natural killer cells from $CD34^+$ hematopoietic progenitor cells. *Blood* 1996. **87:** 2632–2640.

24 **Yu, H., Fehniger, T. A., Fuchshuber, P., Thiel, K. S., Vivier, E., Carson, W. E. and Caligiuri, M. A.,** Flt3 ligand promotes the generation of a distinct $CD34^+$ human natural killer cell progenitor that responds to interleukin-15. *Blood* 1998. **92:** 3647–3657.

25 **Cooper, M. A., Bush, J. E., Fehniger, T. A., VanDeusen, J. B., Waite, R. E., Liu, Y., Aguila, H. L.** *et al.*, *In vivo* evidence for a dependence on interleukin 15 for survival of natural killer cells. *Blood* 2002. **100:** 3633–3638. DOI 10.1182/blood-2001–12–0293.

26 **Domzig, W., Stadler, B. M. and Herberman., R. B.,** Interleukin 2 dependence of human natural killer (NK) cell activity. *J. Immunol.* 1983. **130:** 1970–1973.

27 **Lanier, L. L., Buck, D. W., Rhodes, L., Ding, A., Evans, E., Barney, C. and Phillips, J. H.,** Interleukin 2 activation of natural killer cells rapidly induces the expression and phosphorylation of the Leu-23 activation antigen. *J. Exp. Med.* 1988. **167:** 1572–1585.

28 **Carson, W. E., Giri, J. G., Lindemann, M. J., Linett, M. L., Ahdieh, M., Paxton, R., Anderson, D.** *et al.*, Interleukin (IL) 15 is a novel cytokine that activates human natural killer cells via components of the IL-2 receptor. *J. Exp. Med.* 1994. **180:** 1395–1403.

29 **Harada, H., Saijo, K., Watanabe, S., Tsuboi, K., Nose, T., Ishiwata, I. and Ohno, T.,** Selective expansion of human natural killer cells from peripheral blood mononuclear cells by the cell line, HFWT. *Jpn. J. Cancer Res.* 2002. **93:** 313.

30 **Harada, H., Saijo, K., Ishiwata, I. and Ohno, T.,** A GFP-transfected HFWT cell line, GHINK-1, as a novel target for non-RI activated natural killer cytotoxicity assay. *Hum. Cell* 2004. **17:** 43–48.

31 **Simmons, D. and Seed, B.,** The Fc gamma receptor of natural killer cells is a phospholipid-linked membrane protein. *Nature* 1988. **333:** 568–570.

32 **Phillips, J. H., Hori, T., Nagler, A., Bhat, N., Spits, H. and Lanier, L. L.,** Ontogeny of human natural killer (NK) cells: fetal NK cells mediate cytolytic function and express cytoplasmic CD3 epsilon, delta proteins. *J. Exp. Med.* 1992. **175:** 1055–1066.

33 **Gaddy, J. and Broxmeyer, H. E.,** Cord blood $CD16^+56^-$ cells with low lytic activity are possible precursors of mature natural killer cells. *Cell. Immunol.* 1997. **180:** 132–142.

34 **Harada, H., Watanabe, S., Saijo, K., Ishiwata, I. and Ohno, T.,** A Wilms' tumor cell line, HFWT, can greatly stimulate proliferation of both $CD56^+$ human natural killer cells and their novel precursors in blood mononuclear cells. *Exp. Hematol.* 2004. **32:** 614–621.

35 **Lyons, A. B., and Parish, C. R.,** Determination of lymphocyte division by flow cytometry. *J. Immunol. Methods* 1994. **171:** 131–137.

36 **Grimm, E. A., Mazumder, A., Zhang, H. Z. and Rosenberg, S. A.,** Lymphokine-activated killer cell phenomenon. Lysis of natural killer-resistant fresh solid tumor cells by interleukin 2-activated autologous human peripheral blood lymphocytes. *J. Exp. Med.* 1982. **155:** 1823–1841.

37 **Robertson, M. J., Caligiuri, M. A., Manley, T. J., Levine, H. and Ritz, J.,** Human natural killer cell adhesion molecules: Differential expression after activation and participation in cytolysis. *J. Immunol.* 1990. **145:** 3194–3201.

38 **Vitale, M., Bottino, C., Sivori, S., Sanseverino, L., Castriconi, R., Marcenaro, E., Augugliaro, R.** *et al.*, NKp44, a novel triggering surface molecule specifically expressed by activated natural killer cells, is involved in non-major histocompatibility complex-restricted tumor cell lysis. *J. Exp. Med.* 1998. **187:** 2065–2072.

39 **Weichold, F. F., Jiang, Y. Z., Dunn, D. E., Bloom, M., Malkovska, V., Hensel, N. F. and Barrett, A. J.,** Regulation of a graft-versus-leukemia effect by major histocompatibility complex class II molecules on leukemia cells: HLA-DR1 expression renders K562 cell tumors resistant to adoptively transferred lymphocytes in severe combined immunodeficiency mice/nonobese diabetic mice. *Blood* 1997. **90:** 4553–4558.

40 **Kantakamalakul, W., Jaroenpool, J. and Pattanapanyasat, K.,** A novel enhanced green fluorescent protein (EGFP)-K562 flowcytometric method for measuring natural killer (NK) cell cytotoxic activity. *J. Immunol. Methods* 2003. **272:** 189–197.

41 **Miller, J. S., Alley, K. A. and McGlave, P.,** Differentiation of natural killer (NK) cells from human primitive marrow progenitors in a stroma-based long-term culture system: identification of a $CD34^+7^+$ NK progenitor. *Blood* 1994. **83:** 2594–2601.

42 **Aiuti, A, Webb, I. J., Bleul, C., Springer, T. and Gutierrez-Ramos, J. C.,** The chemokine SDF-1 is a chemoattractant for human $CD34^+$ hematopoietic progenitor cells and provides a new mechanism to explain the mobilization of $CD34^+$ progenitors to peripheral blood. *J. Exp. Med.* 1997. **185:** 111–120.

43 **Robertson, M. J.,** Role of chemokines in the biology of natural killer cells. *J. Leukoc. Biol.* 2002. **71:** 173–183.

44 **Ferlazzo, G., Tsang, M. L., Moretta, L., Melioli, G., Steinman, R. M. and Munz, C.,** Human dendritic cells activate resting natural killer (NK) cells and are recognized via the NKp30 receptor by activated NK cells. *J. Exp. Med* 2002. **195:** 343–351.

45 **Nagler, A., Lanier, L. L. Quirt, S. and Phillips, J. H.,** Comparative studies of human FcRIII-positive and negative natural killer cells. *J. Immunol.* 1989. **143:** 3183–3191.

46 **Rosenberg, S. A., Lotze, M. T., Muul, L. M., Leitman, S., Chang, A. E., Ettinghausen, S. E., Matory, Y. L.,** *et al.*, Observations on the systemic administration of autologous lymphokine-activated killer cells and recombinant interleukin-2 to patients with metastatic cancer. *N. Engl. J. Med.* 1985. **313:** 1485–1492.

47 **Khatri, V. P., Fehniger, T. A., Baiocchi, R. A., Yu, F., Shah, M. H., Schiller, D. S., Gould, M.** *et al.*, Ultra low dose interleukin-2 therapy promotes a type

1 cytokine profile *in vivo* in patients with AIDS and AIDS-associated malignancies. *J. Clin. Invest.* 1998. **101**: 1373–1378.

48 **Fehniger, T. A. and Caligiuri, M. A.,** Interleukin 15: biology and relevance to human disease. *Blood* 2001. **97**: 14–32.

49 **Attia, M.A. and Weiss, D. W.,** Immunology of spontaneous mammary carcinomas in mice. V. Acquired tumor resistance and enhancement in strain A mice infected with mammary tumor virus. *Cancer Res.* 1966. **26**: 1787–1800.

Journal of Cellular Physiology

M-CSF-Mediated Macrophage Differentiation but not Proliferation Is Correlated with Increased and Prolonged ERK Activation

SHINYA SUZU,[1] MASATERU HIYOSHI,[1] YUKA YOSHIDOMI,[1] HIDEKI HARADA,[1] MOTOHIRO TAKEYA,[2] FUMIHIKO KIMURA,[3] KAZUO MOTOYOSHI,[3] AND SEIJI OKADA[1]*

[1]*Division of Hematopoiesis, Center for AIDS Research, Kumamoto University, Kumamoto, Japan*

[2]*Department of Cell Pathology, Graduate School of Medical and Pharmaceutical Sciences, Kumamoto University, Kumamoto, Japan*

[3]*Third Department of Internal Medicine, National Defense Medical College, Saitama, Japan*

M-CSF is a cytokine essential for both the proliferation and differentiation of monocytes/macrophages. In this study, we established a new M-CSF-mediated differentiation-inducing system, and examined how the level and duration of the activation of ERK preceded M-CSF-mediated differentiation. TF-1-fms human leukemia cells rapidly proliferated in response to M-CSF. However, in the presence of a phorbol ester, TPA, TF-1-fms cells definitely switched their responsiveness to M-CSF from proliferation to differentiation, as evidenced by a more drastic morphological change and the appearance of cells with a higher level of phagocytic activity. In TF-1-fms cells expressing HIV-1 Nef protein in a conditionally active-manner, both M-CSF-mediated proliferation and M-CSF/TPA-mediated differentiation were inhibited by the activation of Nef. The Nef-active cells showed perturbed patterns of ERK activation. Under the proliferation-inducing conditions (TPA-free), parental or Nef-inactive cells showed modest ERK activation following M-CSF stimulation, whereas Nef-active cells showed an earlier and transient ERK activation, despite a decrease in their proliferation rate. Under the differentiation-inducing conditions, parental or Nef-inactive cells showed increased and prolonged ERK activation following M-CSF stimulation, whereas Nef-active cells showed transient ERK activation. These results supported the idea that the increased and prolonged ERK activation led to M-CSF-mediated macrophage differentiation but not to proliferation.

J. Cell. Physiol. 9999: 1–7, 2007.

Macrophage colony-stimulating factor (M-CSF) is a cytokine that supports both proliferation and differentiation of the cells of monocytic lineage (Roth and Stanley, 1992). The biological effects of M-CSF are mediated by a receptor tyrosine kinase, Fms (Sherr et al., 1985). The binding of M-CSF leads to the autophosphorylation of tyrosine residues in the cytoplasmic domain of Fms and subsequent interactions of the phosphorylated residues with other proteins, resulting in the initiation of multiple pathways (Bourette and Rohrschneider, 2000). Thus, to investigate which pathway leads to the proliferation or differentiation, mutant Fms proteins in which the tyrosine residues are substituted with phenylalanine have been generated and expressed in various cell types, such as NIH3T3 fibroblasts (Roussel et al., 1990), Rat-2 fibroblasts (van der Geer and Hunter, 1993), FDC-P1 myeloid progenitor cells (Bourette et al., 1995) and M1 myeloid cells (Marks et al., 1999). However, because the pathway that is predominantly utilized and whether cells proliferate or differentiate in response to M-CSF depend on the cell type, the exact differences in the signaling events between these distinct cellular responses to M-CSF are still unclear. Culture systems in which the same cells distinctly respond to different stimuli (proliferation versus differentiation) are useful for clarifying this issue. For example, rat neuronal PC12 cells proliferate in response to EGF, whereas stimulation with NGF causes neuronal differentiation (Marshall, 1995). Of importance, studies with this culture system have revealed that the increased and prolonged activation of extracellular signal-regulated kinase (ERK) is critical for the neuronal differentiation of PC12 cells, but not for proliferation (Marshall, 1995). It has been also shown that the increased and prolonged activation of ERK is critical for the differentiation of megakaryocytes (Melemed et al., 1997; Racke et al., 1997) and muscle cells (Gredinger et al., 1998). Furthermore, the functional maturation of macrophages induced by lipopolysaccharide seemed to require increased and prolonged ERK activation (Valledor et al., 2000). However, the role of ERK activation in M-CSF-mediated macrophage differentiation is not fully understood.

In this study, we first attempted to establish a new M-CSF-mediated differentiation-inducing system, using human leukemia TF-1-fms cells which essentially showed a proliferative response to M-CSF (Suzu et al., 1997). We assessed whether 12-*O*-tetradecanoylphorbol 13-acetate (TPA) triggered their differentiation and M-CSF accelerated the process. TPA has been characterized by its ability to induce the differentiation of several leukemia cell lines (Kitamura et al., 1989; Racke et al.,

Contract grant sponsor: Ministry of Health, Labour and Welfare of Japan;
Contract grant number: H16-AIDS-003.

*Correspondence to: Seiji Okada, Division of Hematopoiesis, Center for AIDS Research, Kumamoto University, Honjo 2-2-1, Kumamoto-city, Kumamoto 860-0811, Japan.
E-mail: okadas@kaiju.medic.kumamoto-u.ac.jp

Received 15 June 2006; Accepted 10 January 2006

Published online in Wiley InterScience (www.interscience.wiley.com.), 00 Month 2007.
DOI: 10.1002/jcp.21045

1997; He et al., 1999). We next attempted to clarify whether the increased and prolonged activation of ERK preceded M-CSF-mediated differentiation, by utilizing TF-1-fms cells expressing a conditionally active HIV-1 Nef protein (Suzu et al., 2005). Previously, we showed that Nef activation inhibited the M-CSF-mediated proliferation of TF-1-fms cells but enhanced the activation of ERK following M-CSF treatment (Suzu et al., 2005). Nef is a major determinant of the pathogenicity of HIV-1 (Fackler and Baur, 2002; Peterlin and Trono, 2003; Qiao et al., 2006), and has been shown to bind to and activate Hck, a Src kinase (Saksela et al., 1995; Moarefi et al., 1997). The activation of Hck was one possible molecular mechanism by which Nef caused the inhibition of M-CSF-mediated cell proliferation (Suzu et al., 2005) and the enhancement of ERK activation (Schrager et al., 2002; He et al., 2004). Based on these findings, we carefully examined how Nef affected the M-CSF/TPA-mediated differentiation of TF-1-fms cells and the level/duration of ERK activation in the differentiation-inducing conditions.

Materials and Methods

Cell culture and reagents

TF-1 cells (Kitamura et al., 1989) were routinely cultured with RPMI 1640 medium (Sigma, St. Louis, MO) — 10% fetal calf serum (FCS) in the presence of recombinant human granulocyte/macrophage-CSF (GM-CSF) (2 ng/ml; PeproTech, London, UK). TF-1-fms cells (Suzu et al., 1997) were maintained with RPMI 1640 — 10% FCS in the presence of M-CSF (100 ng/ml; a gift from Morinaga Milk Industry, Kanagawa, Japan) and G418 (200 μg/ml; Life Technologies, Grand Island, NY). TF-1-fms cells expressing the HIV-1 Nef-murine estrogen receptor hormone-binding domain (Nef-ER) fusion protein (TF-1-fms-Nef-ER) (Suzu et al., 2005) were maintained with RPMI 1640 — 10% FCS containing M-CSF, G418, and puromycin (1.5 μg/ml; Sigma). In this system, Nef was basally inactive but its function was inducibly activated by the estrogen analogue, 4-hydroxytamoxifen (4-HT; Sigma) (Suzu et al., 2005). In this study, we also established TF-1 cells expressing the Nef-ER fusion protein with the plasmid pEBB-Nef-ER-IRES-puro (Walk et al., 2005). TF-1-Nef-ER cells were maintained with RPMI 1640 — 10% FCS containing GM-CSF and puromycin. To activate Nef, 4-HT was added to the culture at a final concentration of 1 μM. TPA (Sigma) was added to the culture at a final concentration of 100 ng/ml. PD98059 (ERK kinase inhibitor) and PP2 (Src kinase inhibitor) were purchased from Sigma. U0126 was purchased from Calbiochem (San Diego, CA).

Cell count and viability analysis

The viable cell counts were obtained by enumerating the cells that excluded trypan blue dye on a hemocytometer. The adherent cells were harvested by trypsinization. The viability of cells was also examined with the propidium iodide (PI) exclusion method (Okada et al., 1998). Cells were suspended in phosphate-buffered saline (PBS) containing 0.1% NaN_3, 3% FCS and 2 μg/ml PI. The uptake of PI in each cell was analyzed with a FACSCalibur using Cell Quest Software (Becton Dickinson, Mountain View, CA).

Analyses of expression of Fms and CD204, and phagocytic activity

The cell surface expression of Fms was analyzed by flow cytometry using Flag-tagged M-CSF (Suzu et al., 2005). In brief, cells were incubated with the Flag-tagged M-CSF followed by biotin-labeled anti-Flag M2 antibody (Sigma) and phycoerythrin (PE)-labeled streptavidin (PharMingen, San Jose, CA). The analyses were performed with a FACSCalibur. The cell surface expression of CD204 was determined using anti-CD204-FITC (clone E-5) (Tomokiyo et al., 2002). The phagocytic activity was determined by measuring the uptake of fluorescent microspheres (Fluoresbrite Carboxylate Microspheres, 0.7 μm in diameter, Polysciences, Warrington, PA). Cells cultured on a 6-well tissue culture plate were incubated with the fluorescent microspheres for 5 h and washed with PBS. The cells showing phagocytized particles were analyzed by flow cytometry.

Immunoprecipitation and Western blotting

The immunoprecipitation and Western blotting were performed essentially as described previously (Suzu et al., 2000, 2005). Cells were depleted of M-CSF for 14 h in RPMI 1640 — 10% FCS with or without TPA, and then stimulated with M-CSF for the indicated periods. In selected experiments, 4-HT was added to the culture at the initiation of M-CSF deprivation/TPA pre-treatment. Then, the cells were solubilized with the Nonidet P-40 lysis buffer. The immunoprecipitation was performed with anti-phosphotyrosine mouse IgG conjugated to agarose (PY99; Santa Cruz Biotechnology, Santa Cruz, CA). The antibodies (purchased from Santa Cruz) used for Western blotting were as follows: anti-Fms (C-20), anti-phosphotyrosine (PY99), anti-ERK (K-23), and anti-phosphorylated ERK (E-4). The rabbit antiserum to Nef was obtained from the NIH AIDS Research and Reference Reagent Program (Division of AIDS, NIAID, NIH[21]). The detection was performed using the ECL system (Amersham, Buckinghamshire, UK). The relative intensity of bands on scanned gel images was quantified by using the NIH Image software.

Results

Proliferative- and differentiative properties of TF-1-fms cells

TF-1-fms cells were derived from TF-1 cells by introducing the wild-type *c-fms* gene into the parental cells (Fig. 1A). The proliferation of TF-1 and TF-1-fms was entirely dependent on GM-CSF and M-CSF, respectively (Fig. 1B) (Kitamura et al., 1989; Suzu et al., 1997). TF-1-fms cells lost their responsiveness to GM-CSF, due to a loss of the expression of the GM-CSF receptor α chain (data not shown). In the presence of M-CSF, TF-1-fms cells neither adhered to dishes (Fig. 1C) nor showed a differentiated morphology (Fig. 1D, top part). On the other hand, when cultured with media containing TPA alone, the cells tended to adhere to dishes and show a flattened morphology (Figs. 1C and D, middle part). Of note, M-CSF accelerated the differentiation-like process. Most TF-1-fms cells cultured in the presence of both M-CSF and TPA adhered to dishes and showed a mature macrophage-like morphology (Figs. 1C and D, bottom part), which closely resembled the primary macrophages obtained by culturing human peripheral blood monocytes with M-CSF (Hashimoto et al., 1999). In parallel with the morphological change, these cells showed more of an increase in granularity than cells cultured with TPA alone (Fig. 1E). More importantly, these cells showed higher phagocytic activity: the percentage of cells phagocytizing the microbeads and their mean fluorescence intensity (MFI) were higher in the culture containing M-CSF and TPA than in the culture containing TPA alone (Fig. 1F, left part). In addition, these cells showed a higher level of CD204 (class A macrophage scavenger receptor) (Fig. 1F, right part). These results indicated that the cells obtained by culturing TF-1-fms cells with both M-CSF and TPA were functionally mature macrophages.
As mentioned above and shown in the upper panel of Figure 2A, the culture of TF-1-fms cells with TPA resulted in the appearance of adherent cells and the addition of M-CSF further increased the number of adherent cells. However, there was no significant difference in total number of viable cells between the two treatments (TPA alone versus M-CSF + TPA) (Fig. 2A, lower part). Moreover, there was no significant difference in the percentage of PI-positive dead cells between the two treatments (Fig. 2B), excluding the possibility that the acceleration of TF-1-fms cell differentiation by M-CSF and TPA reflected a survival-enhancing or anti-apoptotic function of M-CSF. It was therefore likely that TF-1-fms cells definitely switched their responsiveness to M-CSF from proliferation to macrophage differentiation in the presence of TPA.

Requirement of ERK activation for M-CSF-mediated proliferation and M-CSF/TPA-mediated differentiation of TF-1-fms cells

We next examined whether the activation of ERK was required for M-CSF-mediated proliferation and M-CSF/TPA-mediated differentiation of TF-1-fms cells, using pharmacological

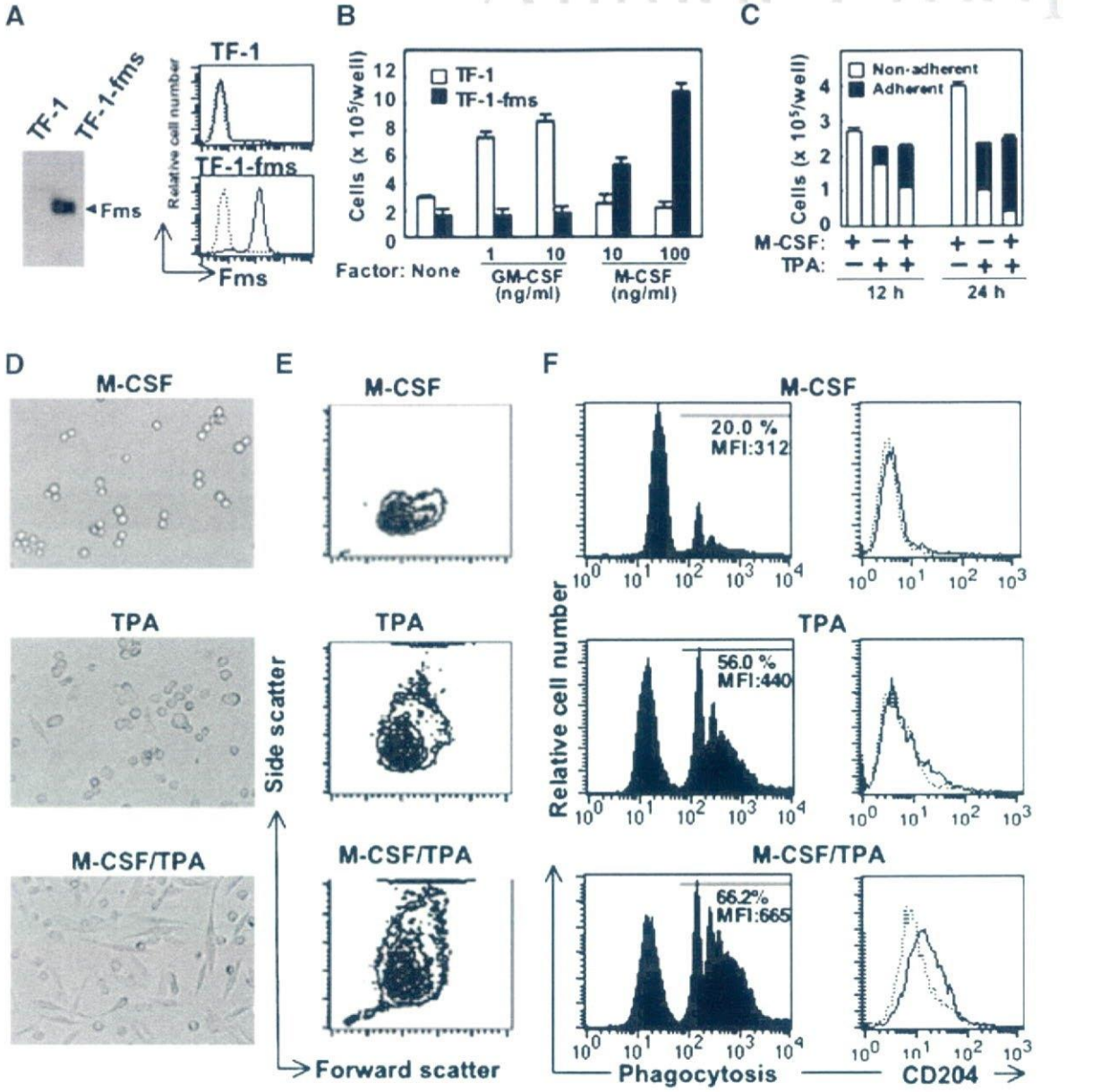

Fig. 1. The expression of Fms in and proliferative and differentiative properties of TF-1-fms cells. A: The total cell lysates from TF-1 or TF-1-fms cells were analyzed for the expression of Fms by Western blotting. Alternatively, the level of cell surface Fms expression was analyzed by flow cytometry with Flag-tagged M-CSF (solid lines). The profiles of cells incubated with a Flag-tagged protein, which is unrelated to M-CSF, are also shown as a control (broken lines). B: TF-1 or TF-1-fms cells were seeded into 6-well culture plates at a density of 5×10^4 cells/ml in the absence or presence of the indicated concentrations of cytokines. TF-1 and TF-1-fms cells were cultured for 3 and 2 days, respectively. After the cultures, viable cells were enumerated. Error bars from triplicate assays are shown. These results are representative of two independent experiments. C: TF-1-fms cells were seeded at a density of 1×10^5 cells/ml, and cultured in the presence of M-CSF, TPA, or both. After culturing for 12 or 24 h, cells adhering to the dishes and non-adherent cells were enumerated. D–F: TF-1-fms cells were seeded at a density of 1×10^5 cells/ml, and cultured for 2 days in the presence of M-CSF (M-CSF), TPA (TPA), or both (M-CSF/TPA). D: The morphology of cells after culturing is shown. The cells cultured with M-CSF alone were photographed after a 5-fold dilution with media. E: The results of flow cytometric analyses of cells for forward and side scatters are shown. An equal number of cells were analyzed and the results are presented as counter plots. F: The phagocytic activity of cells was determined by the procedures described in the Materials and Methods (left panels). The percentage and mean fluorescence intensity (MFI) of cells in the region indicated by solid lines are shown. Alternatively, the cells were analyzed for the expression of CD204 by flow cytometry (right parts).

inhibitors. As shown, PP2 (the inhibitor specific for Src kinases), PD98059 (the inhibitor specific for ERK kinase, MEK), and U0126 (another MEK inhibitor) significantly reduced the rate of M-CSF-mediated proliferation (Fig. 3A). The reduced proliferation rate correlated well with the increase in the percentage of PI-positive dead cells (Fig. 3A). Thus, we could not exclude the possibility that the inhibitory effect of these inhibitors on M-CSF-mediated proliferation reflected their cytotoxicity. Of importance, however, these inhibitors, in particular U0126, significantly inhibited the differentiation of

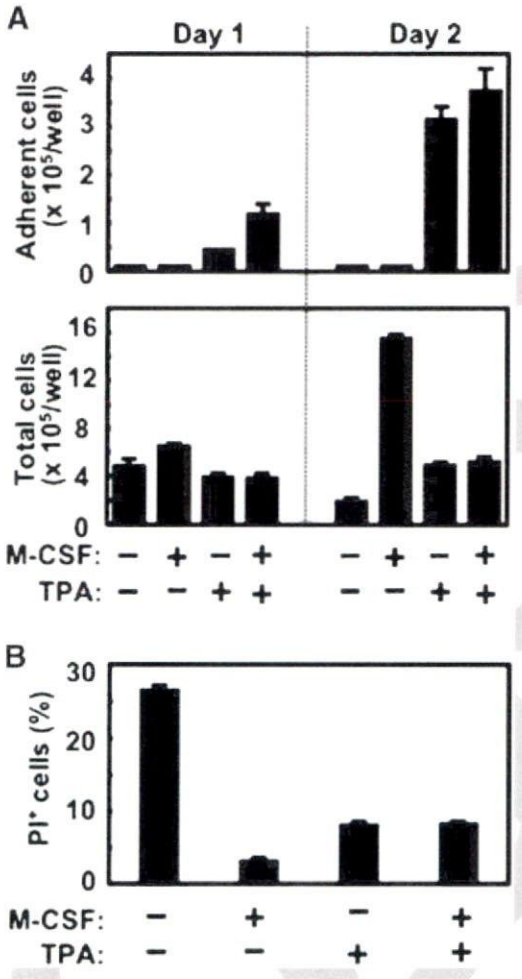

Fig. 2. A comparison of cell viability/death between the culture with TPA alone and that with M-CSF plus TPA. A and B: TF-1-fms cells were seeded into 6-well culture plates at a density of 1×10^5 cells/ml. Then, the cells were cultured in the absence of additives, or the presence of M-CSF, TPA, or both. A: After culturing for 1 or 2 days, cells adhering to the dishes (upper part) and all viable cells (lower part) were enumerated. B: After culturing for 2 days, the percentage of PI-positive dead cells in the wells was determined by flow cytometry. Error bars from triplicate assays are shown. These results are representative of two independent experiments.

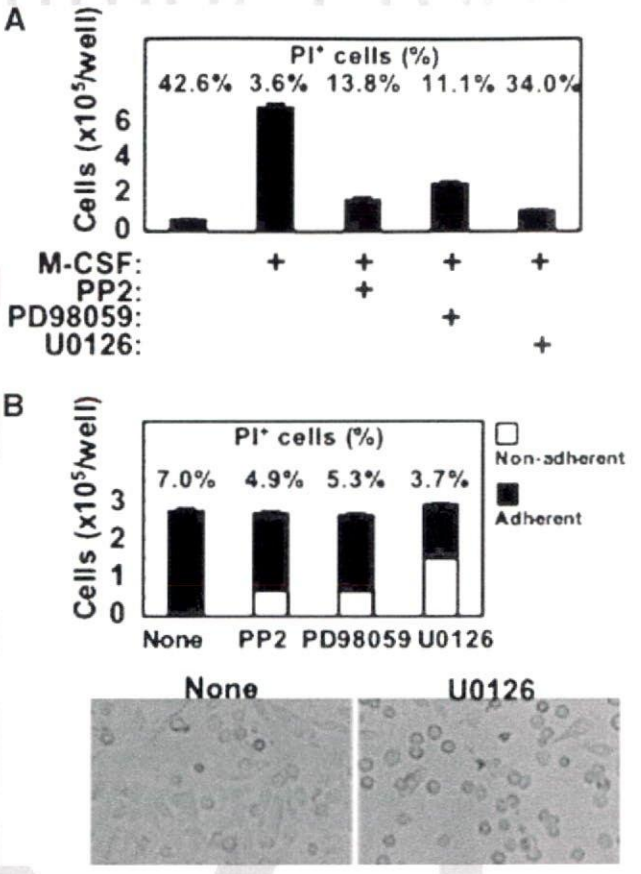

Fig. 3. Effects of pharmacological inhibitors on the proliferation and differentiation of TF-1-fms cells. A: TF-1-fms cells were seeded into 6-well culture plates at a density of 5×10^4 cells/ml in the absence or presence of the indicated inhibitors. M-CSF was added at a final concentration of 100 ng/ml. Both PP2 and U0126 were added at a final concentration of 10 μM. PD98059 was used at a final concentration of 50 μM. After culturing for 2 days, viable cells were enumerated. Error bars from triplicate assays are shown. Simultaneously, the percentage of PI-positive dead cells was determined by flow cytometry. These results are representative of two independent experiments. B: TF-1-fms cells were suspended at 1×10^5 cells/ml in medium containing M-CSF and TPA, and then cultured for 1 day in the absence or presence of the indicated inhibitors. The cells adhering to the dishes and non-adherent cells were enumerated. Error bars from triplicate assays are shown. Simultaneously, the percentage of PI-positive dead cells was determined by flow cytometry. These results are representative of two independent experiments. The morphology of cells after culturing is shown.

TF-1-fms cells induced by M-CSF and TPA without increasing the percentage of PI-positive dead cells (Fig. 3B). These results indicated that the differentiation of TF-1-fms cells was dependent on the activation of ERK.

The level and duration of ERK activation in parental TF-1-fms cells

We next examined whether the increased and/or prolonged activation of ERK preceded the differentiation. We pretreated TF-1-fms cells with TPA or left them untreated, stimulated then with M-CSF or left them un-stimulated, and analyzed the activation of ERK by using an antibody specific for phosphorylated ERK (Fig. 4). Consistent with an earlier report (He et al., 1999), the treatment of TF-1-fms cells with TPA led to the ERK activation (Figs. 4A and B). Following M-CSF stimulation, a number of molecules were shown to be rapidly tyrosine-phosphorylated in both TPA-pretreated cells and untreated cells (Fig. 4A). The most prominent band at 150–160 kD, the tyrosine-phosphorylation level of which was reduced in the pretreated cells, seemed to be Fms (Suzu et al., 2005). The reduction of Fms phosphorylation in the pretreated cells was likely to be due to the reduced cell surface expression of Fms, because the pretreatment caused an increase in the intracellular form of Fms (gp130) and concomitant decrease in the cell surface form of Fms (gp150) (Fig. 4A), as seen in TPA-treated p388D1 macrophages (Wilhelmsen and van der Geer, 2004). Despite the reduced Fms phosphorylation, the level of ERK activation following M-CSF stimulation in TPA-pretreated cells was higher than that in untreated cells (Figs. 4A and B). Although the higher level of ERK activation following M-CSF stimulation seemed to be due to the high baseline level (Fig. 4A, the bar graph), the extent of the activation apparently correlated with the differentiation of TF-1-fms cells.

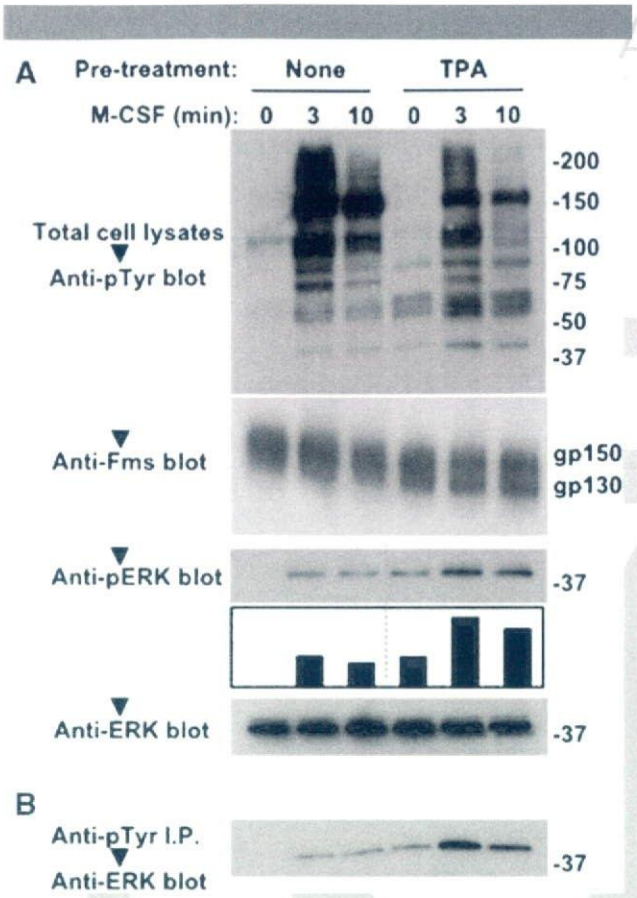

Fig. 4. The level of phosphorylation of ERK in TF-1-fms cells after pre-treatment with TPA and re-stimulation with M-CSF. TF-1-fms cells were deprived of M-CSF with or without TPA for 14 h and then re-stimulated with M-CSF for the indicated periods. A: Total cell lysates were analyzed with Western blotting using an antibody specific for phosphotyrosine (pTyr), Fms, phosphorylated ERK (pERK), or total ERK. The bottom blot was to show that comparable amounts of proteins were loaded in the upper blots. The relative intensities of bands on scanned gel images were quantified using the NIH Image software and the level of phosphorylated ERK normalized to the total amount of ERK is shown in the bar graph. B: The immunoprecipitates with anti-pTyr antibody were analyzed using anti-ERK antibody.

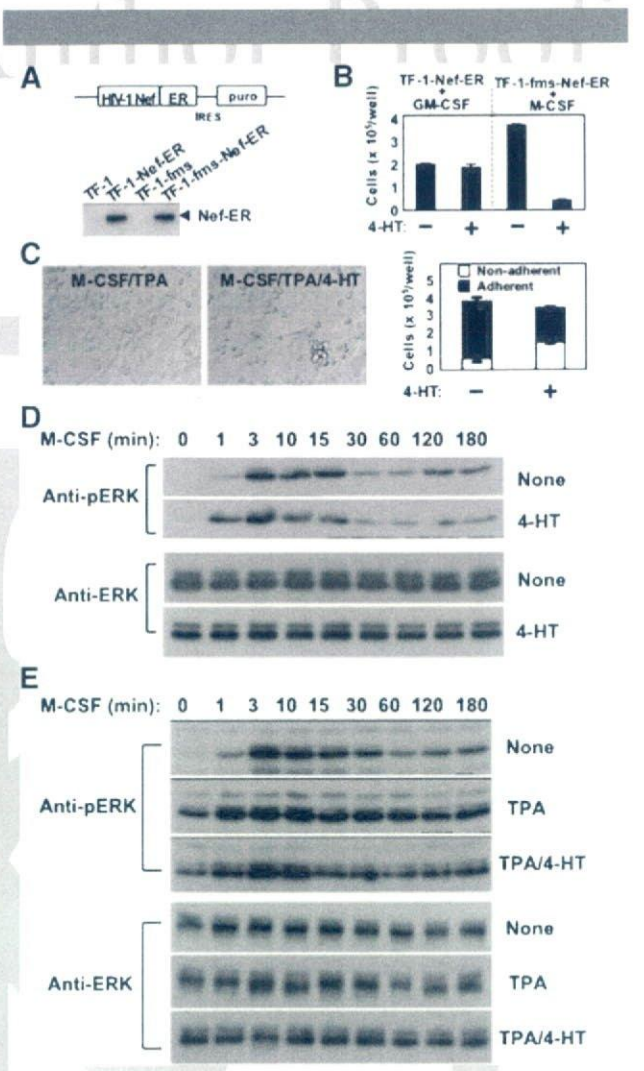

Fig. 5. Establishment of cells expressing the conditionally active Nef, proliferative/differentiative properties, and ERK activation. A: Schematic diagram of the Nef-ER-IRES-puro construct. ER, estrogen receptor hormone-binding domain; IRES, internal ribosomal entry sequence; puro, puromycin resistance gene. Total cell lysates from parental cells (TF-1 and TF-1-fms) or cells stably expressing Nef-ER (TF-1-Nef-ER and TF-1-fms-Nef-ER) were analyzed for the expression of Nef-ER by Western blotting with anti-Nef antibody. B: TF-1-Nef-ER cells were seeded at a density of 2×10^4 cells/ml and cultured in the presence of GM-CSF alone or GM-CSF plus 4-HT for 4 days. Similarly, TF-1-fms-Nef-ER cells were seeded at a density of 1×10^4 cells/ml and cultured in the presence of M-CSF alone or M-CSF plus 4-HT for 4 days. After the cultures, viable cells were enumerated. Error bars from triplicate assays are shown. These results are representative of two independent experiments. C: TF-1-fms-Nef-ER cells were suspended in medium containing M-CSF and TPA, and then cultured for 2 days in the absence (M-CSF/TPA) or the presence of 4-HT (M-CSF/TPA/4-HT). The cells adhering to the dishes and non-adherent cells were enumerated. Error bars from triplicate assays are shown. These results are representative of two independent experiments. D: TF-1-fms-Nef-ER cells were deprived of M-CSF for 14 h and then re-stimulated with M-CSF for the indicated periods. 4-HT was added to the culture at the beginning of the period of deprivation. Total cell lysates were prepared and analyzed by Western blotting using the antibody specific for phosphorylated ERK (upper part) or anti-total ERK antibody (lower part). E: As in D, TF-1-fms-Nef-ER cells were deprived of M-CSF for 14 h and then re-stimulated with M-CSF for the indicated periods. TPA or 4-HT was added to the culture at the beginning of the period of deprivation, as indicated. Total cell lysates were analyzed by Western blotting using the antibody specific for phosphorylated ERK (upper part) or anti-total ERK antibody (lower part). The result is representative of two independent experiments.

The proliferative/differentiative properties and the level/duration of ERK activation in TF-1-fms cells expressing conditionally active HIV-1 Nef

As mentioned above, we previously established TF-1-fms cells expressing the conditionally active HIV-1 Nef protein (the Nef-ER fusion protein) and showed that the activation of Nef by 4-HT caused the inhibition of the M-CSF-mediated proliferation of TF-1-fms cells (Figs. 5A and B; Suzu et al., 2005). By using the newly established TF-1 cells expressing the Nef-ER (Fig. 5A), we excluded the possibility that the inhibitory effect of Nef was due to non-specific cytotoxic activity of the viral protein: the activation of Nef did not affect GM-CSF-mediated proliferation of TF-1 cells (Fig. 5B). In this study, we found that Nef activation also caused the inhibition of the M-CSF/TPA-mediated differentiation of TF-1-fms cells (Fig. 5C). Consistent with its inhibitory effect on both M-CSF-mediated proliferation and M-CSF/TPA-mediated differentiation, Nef perturbed the patterns of ERK activation following the stimulation of TF-1-fms-Nef-ER cells with M-CSF (Figs. 5D and E). The untreated control cells

showed a biphasic ERK activation following M-CSF treatment. The early phase occurred between 1 and 3 min whereas the late phase started after 120 min (Fig. 5D). In contrast, the Nef-active cells whose proliferation rate was low showed an earlier but transient ERK activation following M-CSF stimulation (Fig. 5D). On the other hand, TPA-pretreated cells showed an increased and prolonged activation following M-CSF treatment when compared to the untreated control cells (Fig. 5E). Of importance, however, the Nef-active TPA-pretreated cells showed a transient ERK activation (Fig. 5E). These results suggested that the increased and prolonged activation of ERK correlated well with M-CSF/TPA-mediated differentiation, but not with M-CSF-mediated proliferation, of TF-1-fms cells.

Discussion

We established a new macrophage differentiation-inducing system that was dependent on M-CSF activity. TF-1-fms cells definitely switched their responsiveness to M-CSF from proliferation to differentiation in the presence of TPA (Fig. 1). Although the treatment with TPA alone triggered the macrophage differentiation of the cells, the presence of M-CSF enhanced the process: (1) the combination of both M-CSF and TPA caused more drastic morphological changes (Figs. 1C and D); (2) the culture in the presence of both M-CSF and TPA contained more adherent cells than that in the presence of TPA alone (Fig. 2A, upper part); (3) the phagocytic activity and the expression of CD204 were significantly higher in cells treated with M-CSF and TPA than those treated with TPA alone (Fig. 1E). The macrophage differentiation by M-CSF and TPA did not reflect the survival-enhancing/anti-apoptotic function of M-CSF (Fig. 2A, lower part and B).

The experiments with the pharmacological inhibitor U0126 showed that M-CSF/TPA-mediated differentiation of TF-1-fms was dependent on ERK activation (Fig. 3B). That the Src inhibitor PP2 was also a potent inhibitor of the responses (Fig. 3B) might reflect the finding that the activation of ERK by M-CSF was in part dependent on the activity of Src kinases (Cheng et al., 1999; McMahon et al., 2001). However, the involvement of the increased and/or prolonged ERK activation in M-CSF-mediated differentiation is somewhat controversial. Unlike murine M1 cells expressing wild-type Fms, the cells expressing Y559F mutant Fms showed an impaired differentiative response to M-CSF and a reduced level of ERK activation (McMahon et al., 2001). The enforced expression of a scaffolding protein, Gab2, in wild-type Fms-expressing FDC-P1 cells resulted in an acceleration of the differentiation process and increased ERK activation (Liu et al., 2001). In contrast, the enforced expression of an adapter protein, Mona, in wild-type Fms-expressing FDC-P1 cells resulted in increased and prolonged ERK activation, but not an acceleration of M-CSF-mediated differentiation (Bourgin et al., 2000). Moreover, 32D myeloid cells expressing the Y559F mutant Fms showed a "hyper-proliferative" response to M-CSF and prolonged ERK activation (Rohde et al., 2004). Our studies with parental and Nef-expressing TF-1-fms cells (Figs. 4 and 5) supported the former idea that increased and prolonged ERK activation led to M-CSF-mediated macrophage differentiation, but not to cell proliferation. The TPA-pretreated parental TF-1-fms cells (differentiative) showed increased and prolonged ERK activation following M-CSF stimulation (Fig. 4). In contrast, the Nef-active TPA-pretreated TF-1-fms (un-differentiative) showed transient ERK activation (Figs. 5C and E). The pharmacological agent GF109203X, a potent inhibitor of the expression of MAPK phosphatase-1 (Valledor et al., 1999), caused TF-1-fms cells to differentiate in the presence of M-CSF and the cells pretreated with GF109203X showed a sustained ERK activation following M-CSF treatment (data not shown), further supporting the idea.

The molecular mechanisms whereby Nef inhibited the M-CSF-mediated proliferation and M-CSF/TPA-mediated differentiation of TF-1-fms cells remained to be elucidated. In TF-1-fms cells, Nef activation induced the activation of Hck and its constitutive association with Fms (Suzu et al., 2005). The unphysiological behavior of Hck might explain the inhibitory effect of Nef on the responsiveness to M-CSF. Yet, under the proliferation-inducing conditions (TPA-free), the activation of Nef resulted in an earlier ERK activation (Fig. 5D). This might be explained by the finding that Nef induced ERK activation in $CD4^+$ T cells (Schrager et al., 2002) and podocytes (He et al., 2004) in a Src-dependent manner. Further experiments are required to understand the molecular mechanisms whereby Nef rapidly terminated ERK activation in the presence of TPA (Fig. 5E). In summary, we showed that M-CSF-mediated macrophage differentiation, but not proliferation was correlated with increased and prolonged ERK activation, by using a newly established macrophage-inducing system. The culture system with Nef-expressing TF-1-fms cells provides a useful tool for determining the temporal regulatory mechanism of ERK activation and its contribution to M-CSF-mediated proliferation/differentiation.

Acknowledgments

We thank Ranko Shimamura and Yuka Endo for technical and secretarial assistance, respectively.

Literature Cited

Bourette RP, Rohrschneider LR. 2000. Early events in M-CSF receptor signaling. Growth Factors 17:155–166.

Bourette RP, Myles GM, Carlberg K, Chen AR, Rohrschneider LR. 1995. Uncoupling of the proliferation and differentiation signals mediated by the murine macrophage colony-stimulating factor receptor expressed in myeloid FDCP-1 cells. Cell Growth Diff 6:631–645.

Bourgin C, Bourette R, Mouchiroud G, Arnaud S. 2000. Expression of Mona (monocytic adapter) in myeloid progenitor cells results in increased and prolonged MAP kinase activation upon macrophage colony-stimulating factor stimulation. FEBS Lett 480:113–117.

Cheng M, Wang D, Roussel MF. 1999. Expression of c-Myc in response to colony-stimulating factor-1 requires mitogen-activated protein kinase kinase-1. J Biol Chem 274:6553–6558.

Fackler OT, Baur AS. 2002. Live and let die: Nef functions beyond HIV replication. Immunity 16:493–497.

Gredinger E, Gerber AN, Tamir Y, Tapscott SJ, Bengal E. 1998. Mitogen-activated protein kinase pathway is involved in the differentiation of muscle cells. J Biol Chem 273:19436–10444.

Hashimoto S, Suzuki T, Dong HY, Yamazaki N, Matsushima K. 1999. Serial analysis of gene expression in human monocytes and macrophages. Blood 94:837–844.

He H, Wang X, Gorospe M, Holbrook NJ, Trush MA. 1999. Phorbol ester-induced mononuclear cell differentiation is blocked by the mitogen-activated protein kinase kinase (MEK) inhibitor PD98059. Cell Growth Diff 10:307–315.

He JC, Husain M, Sunamoto M, D'Agati VD, Klotman ME, Iyengar R, Klotman PE. 2004. Nef stimulates proliferation of glomerular podocytes through activation of Src-dependent Stat3 and MAPK1, 2 pathways. J Clin Invest 114:643–651.

Kitamura T, Tange T, Terasawa T, Chiba S, Kuwaki T, Miyagawa K, Piao YF, Miyazono K, Urabe A, Takaku F. 1989. Establishment and characterization of a unique human cell line that proliferates dependently on GM-CSF, IL-3, or erythropoietin. J Cell Physiol 140:323–334.

Liu Y, Jenkins B, Shin JL, Rohrschneider LR. 2001. Scaffolding Gab2 mediates differentiation signaling downstream of Fms receptor tyrosine kinase. Mol Cell Biol 21:3047–3056.

Marks DC, Csar XF, Wilson NJ, Novak U, Ward AC, Kanagasundarum V, Hoffmann BW, Hamilton JA. 1999. Expression of a Y559F mutant CSF-1 receptor in M1 myeloid cells: a role of Src kinases in CSF-1 receptor-mediated differentiation. Mol Cell Biol Res Commun 1:144–152.

Marshall CJ. 1995. Specificity of receptor tyrosine kinase signaling: transient versus sustained extracellular signal-regulated kinase activation. Cell 80:179–185.

McMahon K-E, Wilson NJ, Marks DC, Beecroft TL, Whitty GA, Hamilton JA, Csar XF. 2001. Colony-stimulating factor-1 (CSF-1) receptor-mediated macrophage differentiation in myeloid cells: a role for tyrosine 559-dependent protein phosphatase 2A (PP2A) activity. Biochem J 358:431–436.

Melemed AS, Ryder JW, Vik TA. 1997. Activation of the mitogen-activated protein kinase pathway is involved in and sufficient for megakaryocytic differentiation of CMK cells. Blood 90:3462–3470.

Moarefi I, LaFevre-Bernt M, Sicheri F, Huse M, Lee C-H, Kuriyan J, Miller WT. 1997. Activation of the Src-family tyrosine kinase Hck by SH3 domain replacement. Nature 385:650–653.

Okada S, Zhang H, Hatano M, Tokuhisa T. 1998. A physiological role of Bcl-$_{xL}$ induced in activated macrophages. J Immunol 160:2590–2596.

Peterlin BM, Trono D. 2003. Hide, shield and strike back: how HIV-infected cells avoid immune eradication. Nat Rev Immunol 3:97–107.

Qiao X, He B, Chiu A, Knowles DM, Chadburn A, Cerutti A. 2006. Human immunodeficiency virus 1 Nef suppresses CD40-dependent immunoglobulin class switching in bystander B cells. Nat Immunol 7:302–310.

Racke FK, Lewandowska K, Goueli S, Goldfarb AN. 1997. Sustained activation of the extracellular signal-regulated kinase/mitogen-activated protein kinase pathway is required for megakaryocytic differentiation of K562 cells. J Biol Chem 272:23366–23370.

Rohde CM, Schrum J, Lee AW-M. 2004. A juxtamembrane tyrosine in the colony stimulating factor-1 receptor regulates ligand-induced Src association, receptor kinase function, and down-regulation. J Biol Chem 279:43448–43461.

Roth P, Stanley ER. 1992. The biology of CSF-1 and its receptor. Curr Top Microbiol Immunol 181:141–167.

Roussel MF, Shurtleff SA, Downing JR, Sherr CJ. 1990. A point mutation at tyrosine-809 in the human colony-stimulating factor 1 receptor impairs mitogenesis without abrogating tyrosine kinase activity, association with phosphatidylinositol 3-kinase, or induction of *c-fos* and *junB* genes. Proc Natl Acad Sci USA 87:6738–6742.

Saksela K, Cheng G, Baltimore D. 1995. Proline-rich (PxxP) motifs in HIV-1 Nef bind to SH3 domains of a subset of Src kinases and are required for the enhanced growth of Nef^+ viruses but not for down-regulation of CD4. EMBO J 14:484–491.

Schrager JA, Der Minassian V, Marsh JW. 2002. HIV Nef increases T cell ERK MAP kinase activity. J Biol Chem 277:6137–6142.

Sherr CJ, Rettenmier CW, Sacca R, Roussel MF, Look AT, Stanley ER. 1985. The *c-fms* proto-oncogene product is related to the receptor for the mononuclear phagocyte growth factor, CSF-1. Cell 41:665–676.

Suzu S, Kimura F, Ota J, Motoyoshi K, Itoh T, Mishima Y, Yamada M, Shimamura S. 1997. Biologic activity of proteoglycan macrophage colony-stimulating factor. J Immunol 159:1860–1867.

Suzu S, Tanaka-Douzono M, Nomaguchi K, Yamada M, Hayasawa H, Kimura F, Motoyoshi K. 2000. $p56^{dok-2}$ as a cytokine-inducible inhibitor of cell proliferation and signal transduction. EMBO J 19:5114–5122.

Suzu S, Harada H, Matsumoto T, Okada S. 2005. HIV-1 Nef interferes with M-CSF receptor signaling through Hck activation and inhibits M-CSF bioactivities. Blood 105:3230–3237.

Tomokiyo R, Jinnouchi K, Honda M, Wada Y, Hanada N, Hiraoka T, Suzuki H, Kodama T, Takahashi K, Takeya M. 2002. Production, characterization, and interspecies reactivities of monoclonal antibodies against human class A macrophage scavenger receptors. Atherosclerosis 161:123–132.

Valledor AF, Xaus J, Marques L, Celeda A. 1999. Macrophage colony-stimulating factor induces the expression of mitogen-activated protein kinase phosphatase-1 through a protein kinase C-dependent pathway. J Immunol 163:2452–2462.

Valledor AF, Comalada M, Xaus J, Celeda A. 2000. The differential time-course of extracellular-regulated kinase activity correlates with the macrophage response toward proliferation or activation. J Biol Chem 275:7403–7409.

van der Geer P, Hunter T. 1993. Mutation of Tyr697, a GRB2-binding site, and Tyr721, a PI 3-kinase binding site, abrogates signal transduction by the murine CSF-1 receptor expressed in Rat-2 fibroblasts. EMBO J 12:5161–5172.

Walk SF, Alexander M, Maier B, Hammarskjold M-L, Rekosh DM, Ravichandran KS. 2001. Design and use of an inducibly activated immunodeficiency virus type 1 Nef to study immune modulation. J Virol 75:834–843.

Wilhelmsen K, van der Geer P. 2004. Phorbol 12-myristate 13-acetate-induced release of the colony-stimulating factor 1 receptor cytoplasmic domain into the cytosol involves two separate cleavage events. Mol Cell Biol 24:454–464.

Q1: Author: Please provide complete location.

Q2: Author: Please cite the reference in the text